

Quantifying Contact-Electrification Induced Charge Transfer on a Liquid Droplet after Contacting with a Liquid or Solid

Zhen Tang, Shiquan Lin, and Zhong Lin Wang*

Contact electrification (CE) is a common physical phenomenon, and its mechanisms for solid–solid and liquid–solid cases have been widely discussed. However, the studies about liquid–liquid CE are hindered by the lack of proper techniques. Here, a contactless method is proposed for quantifying the charges on a liquid droplet based on the combination of electric field and acoustic field. The liquid droplet is suspended in an acoustic field, and an electric field force is created on the droplet to balance the acoustic trap force. The amount of charges on the droplet is thus calculated based on the equilibrium of forces. Further, the liquid–solid and liquid–liquid CE are both studied by using the method, and the latter is focused. The behavior of negatively precharged liquid droplet in the liquid–liquid CE is found to be different from that of the positively precharged one. The results show that the silicone oil droplet prefers to receive negative charges from a negatively charged aqueous droplet rather than positive charges from a positively charged aqueous droplet, which provides a strong evidence about the dominant role played by electron transfer in the liquid–liquid CE.

1. Introduction

Contact electrification (CE) is a widely-known physical phenomenon, but its mechanism has been discussed for decades without a definitive conclusion. This may be due to the lack of proper techniques to measure the charge transfer in CE, especially for the liquid–liquid cases. In traditional studies about solid–solid CE, the static charges induced by CE on the solid surface were usually measured based on electrostatic induction effect.^[1] When a solid surface is contacted by another solid surface, the transferred charges on the solid surface will induce an electrical signal on the back electrode, and the charge density

on the solid surface can be further calculated.^[2] Recently, Kelvin probe force microscopy (KPFM) was also demonstrated to be a powerful tool for studying the solid–solid CE^[3] even liquid–solid CE.^[4] The studies based on KPFM provide some important clues to reveal the electron transfer mechanism of the CE. In contrast, although some previous literatures reported on the CE between liquid and liquid, because majority of reports measured the exchange charge at liquid–liquid interface based on the electrochemical principles, the influence of the reaction container on it cannot be ruled out,^[5] physical method for probing the charges of liquid droplet in the CE still remains challenging, due to difficulty in liquid–liquid separation and the fluidity of the liquids. However, liquid–liquid CE is an equally important physical phenomenon in both science and technology

as the solid–solid and liquid–solid CE. It was reported that the triboelectric nanogenerator (TENG) can be designed based on liquid–liquid CE for energy harvesting,^[6] which ignited an interest in probing liquid–liquid CE. Therefore, it is urgent and important to design a method to quantify the charges on a liquid droplet and further to study the liquid–liquid CE.

A very famous experiment in the history of physics provides an inspiration for quantifying charges of on liquid droplet. Millikan levitated the charged oil droplets in the electric field and determined the charge quantity of a single electron.^[7] It was reported that acoustic levitation technology can levitate liquid droplets, and further widely utilized to study areas include manipulation of subject,^[8] chemical reaction,^[9] material analysis,^[10] etc. Except for liquid–liquid case, some studies using acoustic levitation to study CE between solids and solids,^[11] solids and liquids^[12] have been reported. We realized that the liquid droplet can be suspended in air to avoid contacting with solids and introducing extra charges^[13] in the CE experiments. In this technique, a fixed-frequency wave is generated by using ultrasonic transducers to forming a standing wave, and traps a tiny liquid droplet at the wave node freely. Moreover, the acoustic trap force on the droplet can be precisely calculated and experimentally calibrated. If the droplet is charged, a force can be created on the droplet by applying an electric field against the acoustic trap force. By calculating the acoustic trap force, the electric field force on the droplet can be obtained based on the equilibrium of force, and further calculating the amount of charges on the liquid droplet.

Z. Tang, S. Lin, Z. L. Wang
Beijing Institute of Nanoenergy and Nanosystems
Chinese Academy of Sciences
Beijing 100083, P. R. China
E-mail: zlwang@gatech.edu

Z. Tang, S. Lin
School of Nanoscience and Technology
University of Chinese Academy of Sciences
Beijing 100049, P. R. China

Z. L. Wang
School of Materials Science and Engineering
Georgia Institute of Technology
Atlanta, GA 30332-0245, USA

 The ORCID identification number(s) for the author(s) of this article can be found under <https://doi.org/10.1002/adma.202102886>.

DOI: 10.1002/adma.202102886

In this paper, we propose a contactless method for in situ measuring the amount of charges on a liquid droplet based on the combination electric field and acoustic field. The behavior of charge transfers at the liquid–solid and the liquid–liquid interface was systematically studied, and the relationship between the evaporation of droplets and the residual charges was also discussed based on the proposed method. It is noticed that the oil droplet prefers to receive negative charges from a prenegatively charged aqueous droplet, rather than positive charges from a prepositively charged aqueous droplet, which gives a potential clue about the existence of electron transfer in the liquid–liquid CE.

2. Results

2.1. Working Mechanism of the Acoustic Levitation for Droplet Charge Measurement

As shown in Figure 1a, an acoustic levitation device, which is composed of 72 ultrasonic transducers, can generate standing waves, and the droplets can be trapped at the wave nodes of the acoustic field so that it is freely suspended without any contact with the environmental objects. According to the location of the ultrasonic transducers, the distribution of the sound pressure in the acoustic field can be calculated based on previous reports,^[14] as shown in Figure 1b. Further, the Gorkov potential (U)^[15] in the acoustic field can be also obtained, and the acoustic field force is the negative gradient of the Gorkov potential, as shown below

$$F_a = -\nabla U \quad (1)$$

A pair of parallel plate electrodes are placed on the left- and right-hand sides of the liquid droplet for generating an approximate uniform electric field. If the liquid droplet is charged, an electric field force (F_e) will be created on the liquid droplet. According to the equilibrium of force, the electric field force and the acoustic field force on the liquid droplet should be equal in magnitude and opposite in direction, as following

$$F_e = -F_a \quad (2)$$

where F_a is the component of the acoustic field force on the droplet in the direction of the electric field, and the relation between F_a and the x -position of droplet with different diameters in the acoustic field was calculated by using an open sources software, and the results are shown in Figure 1c. Detailed description about the accuracy of the model and the effects on reflection and nonlinearity were elaborated in previous works.^[14a,16]

Figure 1d–f gives a schematic diagram of the liquid droplet charge measurement. As shown in Figure 1e, the droplet will be trapped in the center position of the acoustic field, when a voltage is applied to the right-hand side electrode and the other is grounded, an electric field will be established, as shown in Figure 1d. If the droplet is positively charged in this case, the droplet will move to the left-hand side dragging by the electric field force until it reaches a position, at which the electric

field force and acoustic force reach equilibrium. The larger the amount of positive charges, the larger the electric field force on the liquid droplet will be, and the farther the droplet moves to the left-hand. If the droplet is negatively charged, the droplet will move to the right-hand side and reach an equilibrium position eventually, as shown in Figure 1f. According to Figure 1c and Equation (2), the acoustic force and electric field force can be obtained by measuring the movement distance of the droplet. Then, the charges of the liquid droplet can be calculated by using following equation

$$Q = \frac{F_e}{E} = \frac{dF_e}{V} \quad (3)$$

where Q is the amount of charges on the liquid droplet, V is the voltage applied on the right-hand side electrode, d is the distance between the two electrodes, and E denotes the electric field induced by the voltage.

We give a demonstration of the measurement method, in which the movement of the liquid droplet is observed by using a camera, as shown in Figure 1g–i, and the experiment processes are shown in Movie S1 (Supporting Information). In Figure 1g, a deionized water (DI water) droplet, which was positively precharged by a metal ring with -5 kV voltage, was trapped in the acoustic field. The detailed description about the process of precharged water see method and (Figure S1, Supporting Information). When $+15$ kV voltage was applied to the right-hand side electrode, the positively charged DI water droplet was dragged to the left-hand side. The distance between the two electrodes was set to be 38 mm, and the movement distance of the droplet was measured to be 1.2 mm by using the camera. According to Figure 1c, the acoustic force was determined to be $705 \mu\text{N}$. Based on the Equations (2) and (3), the positive charges on the DI water droplet in Figure 1g was calculated to be 1788 pC . If there is no electric field between the two electrodes, the droplet will stay at the center of the acoustic field, as shown in Figure 1h. When the DI water droplet was negatively precharged and a $+15$ kV voltage was applied to the right-side electrode, as shown in Figure 1i, the droplet was attracted by the right-hand side electrode. With the same method, the movement of the negatively charged droplet was measured to be 0.7 mm, and the negative charges on the DI water droplet in Figure 1i was calculated to be -10.72 pC . The resolution of the camera used in the experiments is 0.1 mm, so that the sensitivity of this method can minimal up to 1.55 pC , and it can be further optimized by enhancing the electric field or changing the acoustic waves. Comparing to traditional charge measurement method, such as that based on electrostatic induction effect, the acoustic levitation method can measure the transferred charges on the liquid side in the CE, with a basic charge sensitivity (higher than 1.55 pC) and an almost noncontact measurement environment. More importantly, the charge sensitivity measured by this method exceeds the sensitivity of previous methods based on the velocity method^[17] and the droplet trajectory method.^[18] As shown in Figure S2 (Supporting Information), the method in this article and the use of a Faraday cup connected to an electrometer (Keithley 6517B) were also used to measure the amount of charges of water droplets, which carried positive or negative charges. The results show that the two

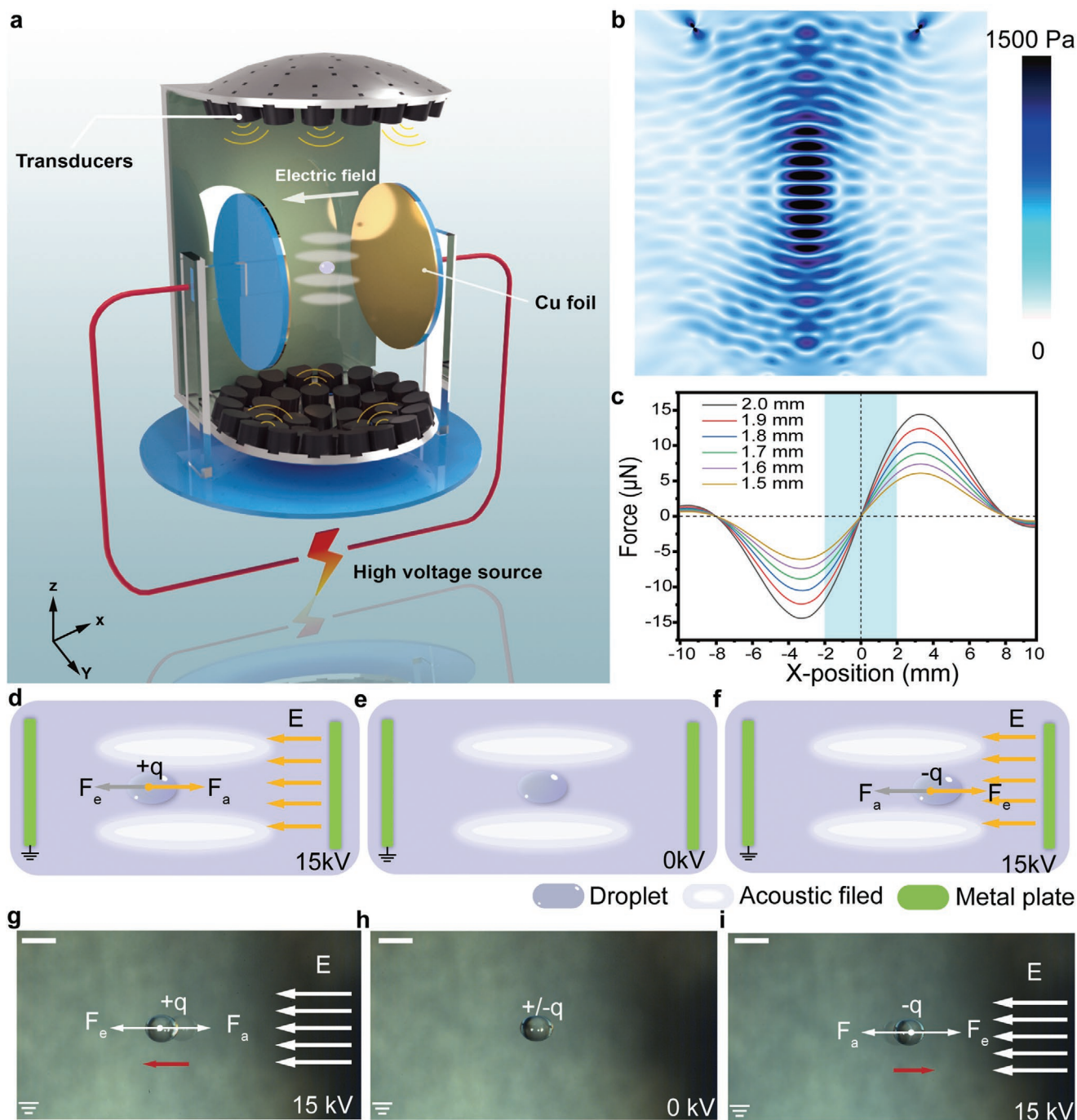


Figure 1. Schematic illustration about the measurement method of charges on a freely suspended liquid droplet. a) Schematic diagram showing experimental setup for directly measuring the quantity of charges carried by the droplet. b) Simulated distribution of acoustic pressure in the acoustic field. c) The acoustic field force on the liquid droplet in x-direction. d–f) schematic diagram of the working principle. e) Charged droplet stably suspends in position due to ambient acoustic force, when electric field is off. Attracted by the electrostatic force d) droplet with negative charges moves toward to the positive plate and f) droplet with positive charges repelled toward the negative plate, when electric field is on. g–i) Photographs of the charge measurement process (The red arrow represents the movement direction of droplets; the image of the shadow represents the original position of the droplet). Scale bar: 2 mm.

methods have obtained the amount of charges are at the same charge level (Figure S2a, Supporting Information), in order to further comparison, the amount of charges carried by the solid after contacting with the droplet was also measured. As shown

in Figure S2b (Supporting Information), the solid has same amount of charges but opposite polarity as the water droplet. The direction of the electric field may affect the test results, as shown in Figure S3 (Supporting Information), by changing the

direction of the electric field, the measurement results were consistent. It demonstrates that the droplet is in the center of the acoustic field and the parallel plate, and the change in the amount of charge is not caused by the polarization of the droplet. The results show that the method proposed in this article possesses a good accuracy. In addition to the liquid–solid and liquid–liquid CE, this method can also be used to study the CE between liquid and gas, solid, and gas, etc. Considering the superiority of this method, it is expected to be a new tool to calibrate the triboelectric properties of liquid or solid materials.

2.2. CE between Liquid and Solid

In order to test the feasibility of the device and charge measurement method, the acoustic levitation device was used to study the CE charge transfer behaviors between solid spheres and liquid droplets. Here, Polytetrafluoroethylene (PTFE), which is widely used in TENG based on solid–liquid CE^[19] and has a good stability and chemical inertness when facing strong acids and bases, is chosen as the solid material. The liquid droplets are from aqueous solutions of different ion concentrations. **Figure 2a** illustrates the contact process between the PTFE sphere and DI water droplet (Movie S2, Supporting Information), in which a DI water droplet is suspended in the acoustic field and a PTFE sphere contacts the DI water droplet then successfully separates. The whole process for the measurement of CE between liquid and solid is shown in **Figure 2b**; and Movie S3 (Supporting Information). For a better comparison, two DI water droplets were trapped in two wave nodes i). When a +15 kV voltage was applied to the right-hand side electrode, the two DI water droplets move to the right-hand side with a small shift before contact with PTFE, which suggests that the initial charges of the two DI water droplets were negative ii). Then, we removed the voltage and contacted the upper DI water droplet with the PTFE sphere for 4 times iii). After the contact iv), the +15 kV voltage was reapplied to the right-hand side electrode. In this case, the upper droplet, which was contacted by the PTFE, shifted to left-hand side, while the other droplet still went right-side under the electric field. This implies that the upper droplet received positive charges after contacting with the PTFE sphere, and the amount of the transferred charges from the PTFE sphere to the DI water is calculated to be about +10.7 pC. Fluorescent dye (Fluorescein sodium salt, aladdin) added in the water were used to characterize the solid–liquid separation process as shown in Movie S4 (Supporting Information). No liquid remains on the solid surface, indicating that the solid–liquid interface can be completely separated.

Further, the effect of the contact number was discussed. As shown in **Figure S4** (Supporting Information), the positive charges in the DI water droplets were found to increase with the increasing of the number of contact cycles. In order to increase the charge transfer, the contact number was set to 20 times in the following experiments. Different solid materials, including PTFE, silicone rubber (Ecoflex00-30) and paraffin were used to contact the DI water droplet, and the amount of the transferred charges from the different solid materials to the DI water droplets is shown in **Figure S5** (Supporting Information). It is noticed that the DI water droplet received highest

positive charges when it contacted with the PTFE, because the PTFE is one of the most electronegative materials here.^[20] Different aqueous solutions were also used in the experiments and the results are shown in **Figure 2c–h**. In **Figure 2c,d** gives the effect of the pH value on the CE between aqueous solutions and PTFE. It is shown that the amount of charges transferred at the solid–liquid interface increases as the concentration of the HCl solution decreases; and also, with the concentration of NaOH solution increases, the amount of transferred charge at the solid–liquid interface decreases. Therefore, the decreasing of transferred charges in the liquid–solid CE may be caused by the increased ion concentration of the liquid droplet, as reported in previous studies.^[21] Therefore, different NaCl solutions with different concentration were used as the liquid droplet in the experiments and the results are shown in **Figure 2e**, it can be seen that the transferred charges from the PTFE sphere to the NaCl solutions decrease with the increasing of the NaCl concentrations. In order to further verify this tendency, Ecoflex was also selected as a solid material to contact with droplets, as shown in **Figure 2f–h**. The results are similar to the above experiment, in which the increasing of ion concentration of the liquid droplet will result in the decreasing of the transferred charges in liquid–solid CE. The above experimental results are in good accordance with the research results reported previously,^[22] the practicability of the device and measurement method is further verified.

2.3. CE between Liquid and Liquid

In addition to the study of liquid–solid CE, the acoustic levitation device can be used to study the CE between liquid and liquid, which is a knotty problem in the study of the CE. As shown in **Figure 3a**, silicone oil, which has a large range of viscosities and lower the standing wave amplitude required,^[23] can be trapped in the acoustic field just liking the DI water droplet (i). Here, a DI water droplet was used to contact the silicone oil droplet. As shown in **Figure 3a(ii–viii)** and Movie S5 (Supporting Information), the silicone oil droplet and DI water droplet seem to be separated well, since water and silicone oil are immiscible.^[24] In order to further investigate the liquid–liquid separation, the characteristics of the oil–water interface have been studied. The measured surface tension of the oil–water interface is shown in **Table S1** (Supporting Information), where γ_{oa} is the interfacial tension between oil and air, γ_{wa} is the interfacial tension between water and air, and γ_{ow} is the interfacial tension between water and oil. The schematic diagram of the surface tension of the water–oil interface according to the Neumann triangle condition is as shown **Figure S6a** (Supporting Information). The calculated spreading coefficient (Sow) is greater than 0, which means that when oil and water contact, the oil will cloak the water.^[25] In the optical picture (**Figure S6b**, Supporting Information) and the fluorescence schematic diagram (**Figure S6c**, Supporting Information), the appearance of the oil ridges can be clearly observed, which proves that the silicone oil will cloak the water when the oil is in contacting with the water droplets, and oil may form an invisible layer covering the water droplet, so it may be possible that oil droplets remain on the water droplets during liquid–liquid separation. In order to better characterize the liquid–liquid

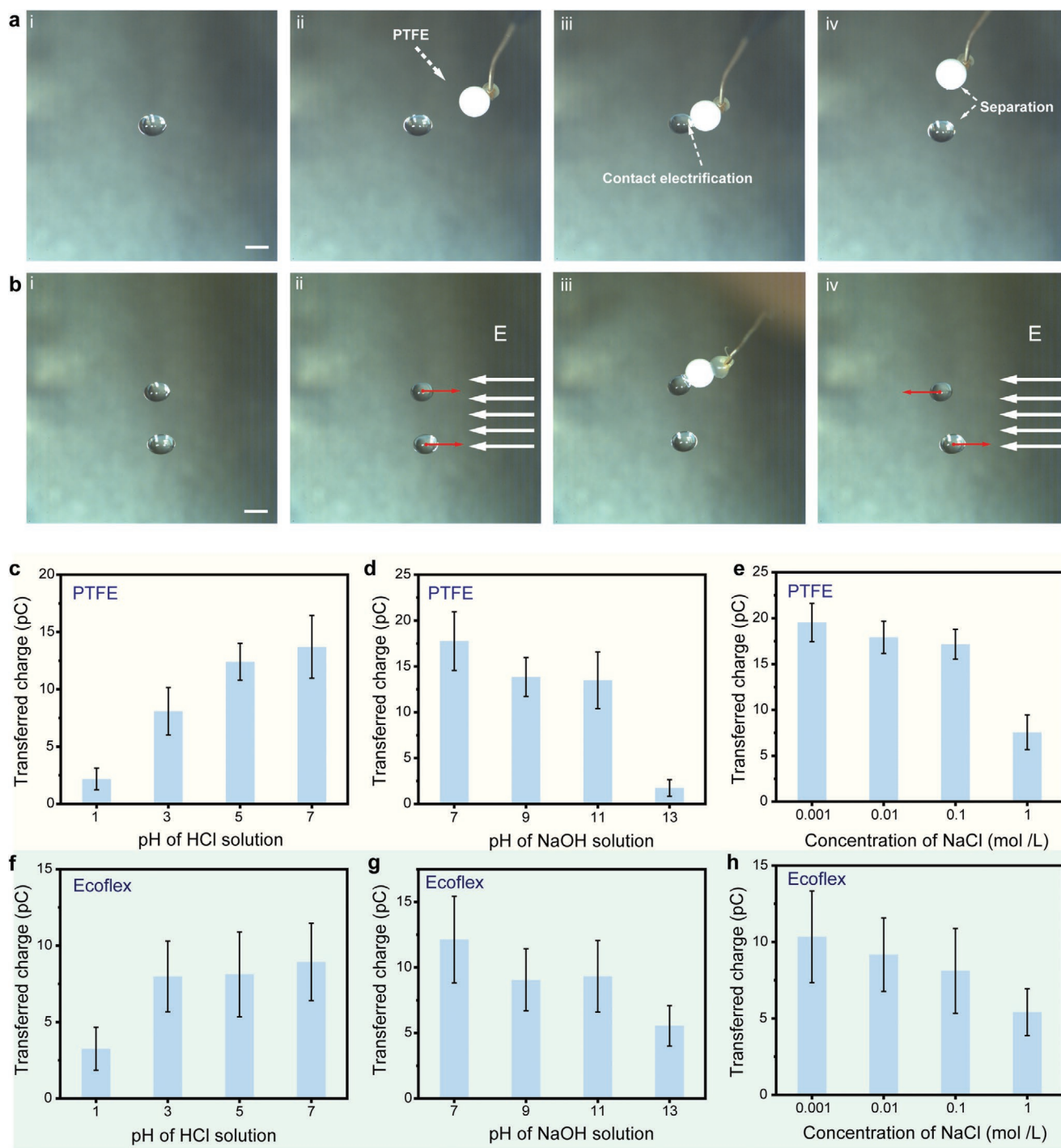


Figure 2. Measuring CE between liquids and solids. a) Photographs of the contact-separation process between a DI water droplet and a solid PTFE. b) Photographs of the whole CE experiments process between a DI water droplet and a solid PTFE. The transferred charges from the PTFE sphere to the c) HCl solutions, d) NaOH solutions and e) NaCl solutions with different concentration. The transferred charges from Ecoflex sphere to the f) HCl solutions, g) NaOH solutions, and h) NaCl solutions with different concentration. Direction of negative charge transfer is from liquids to solids. Error bars represent the standard deviation of ten measurements. Scale bar: 2 mm.

separation, Fluorescein sodium salt and fluorophore Nile Red were added to water and oil, respectively. The liquid–liquid contact separation experiments under dark and bright lighting conditions were performed. Different addition cases of fluorescent tracers were studied. For example, fluorescent dyes were

only added in water (Movie S6, Supporting Information), only added in oil (Movie S7, Supporting Information) and added in oil and water (Movie S8, Supporting Information). Through the comparison of multiple movies, even at the oil–water interface with fluorescent mark, no obvious invisible layer was observed.

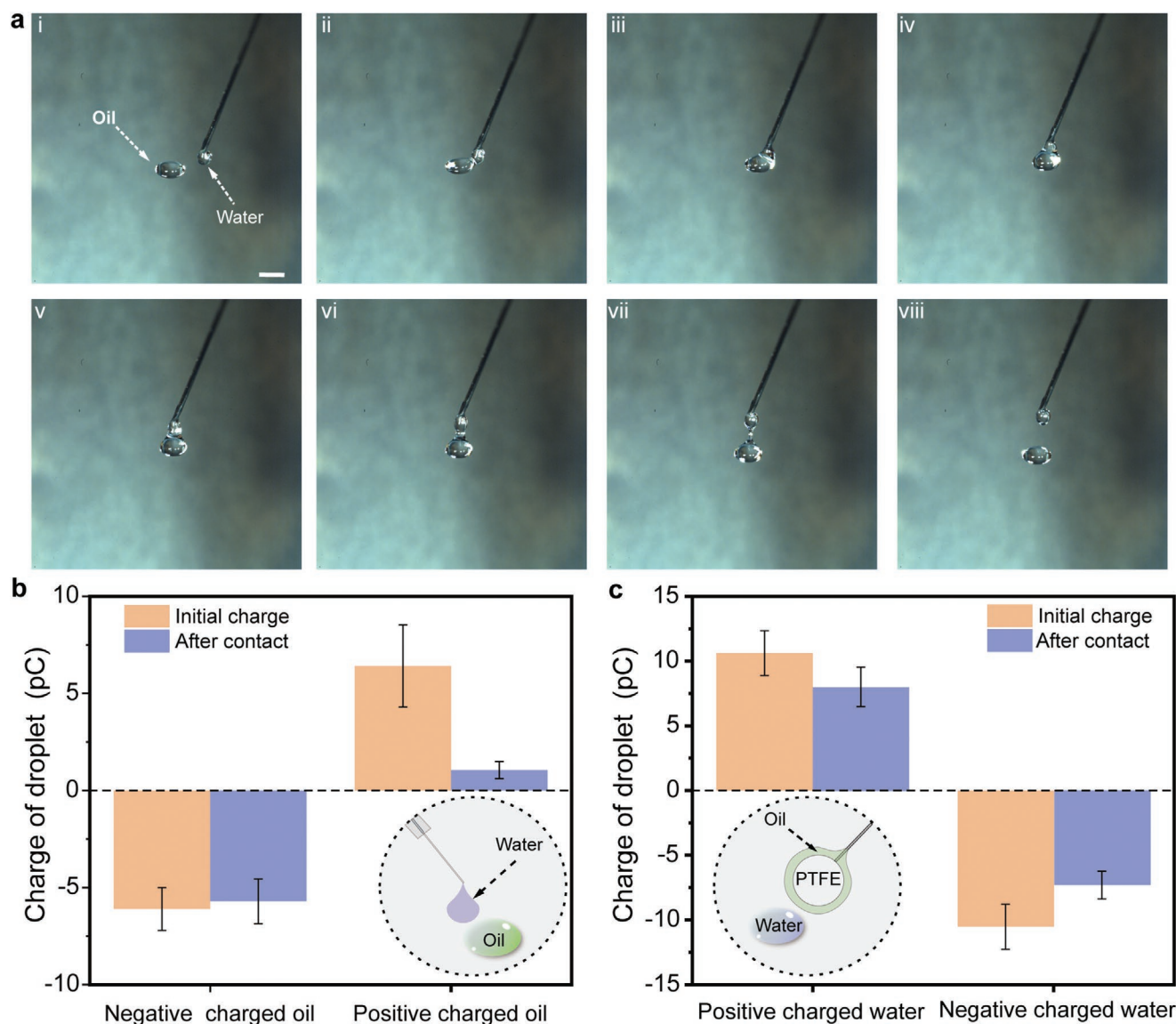


Figure 3. CE between silicone oil droplet and DI water droplet. a) Photographs of the contact and separation between a suspended silicone oil droplet and a DI water droplet. b) The charges on a precharged silicone oil droplet before and after the contact with the DI water. c) The charges on a precharged DI water droplet before and after the contact with the silicone oil. Scale bar: 2 mm.

Because the thickness of the invisible layer may be on the nanometer scale,^[26] it is difficult to determine the existence of the invisible layer, but the possibility of residues still cannot be ruled out, so the real situation of liquid–liquid separation may not appear at the oil–water interface. Instead, oil droplets may separate from the invisible oil layer adsorbed on the droplets. After the contact, the charges of the silicone oil droplet can be quantified by applying an electric field as described above. We found that the transferred charges between liquid and liquid are much less than that between liquid and solid. As shown in Figure S7 (Supporting Information), whether it is from water to oil or oil to water, there is almost no charge transfer between the electrically neutral silicone oil and the electrically neutral water in CE. This may be caused by that the potential barrier at the liquid–liquid interface for electron transition may be higher than that at the solid–solid and liquid–solid interface,

the transfer of charge lacks driving force to overcome the barrier, due to a weaker electron clouds overlap between the two atoms belong to the two liquid molecules.^[27]

In order to observe obvious charge transfer phenomenon and explore the carrier of charge between liquid and liquid, we purposely make droplets precharged by a biased metal ring providing a lot of extra charges or a driving force to overcome the potential barrier of between two liquids. Since free ions always exist in water, it is difficult to distinguish the contribution of electrons and ions to charge transfer. However, the use of ion-free oil can eliminate the effects of ions.^[22b] As shown in Figure 3b, when an ion free silicone oil droplet is initially negatively charged, the amount of charges of the silicone oil droplet is only slightly reduced after contacting with a water droplet. On the contrary, when the silicone oil droplet is positively charged, most of the positive charges carried by silicone oil droplet are

neutralized by the negative charges from DI water droplet during the contact. The conventional notion is that the preferential adsorption of hydroxide ions (OH^-) neutralizes the charges. But by first-principles calculations, a charge transfer mechanism for nonhydroxide ions adsorption is proposed and some spillage of electrons from the oil–water interface to the oil phase is observed.^[28] In order to completely exclude the possible interference of the ions from water dissolved in the oil on the charge transfer, the activated molecular sieve (3A) was used to thoroughly dry the oil before the tests, as shown in Figure S8 (Supporting Information), and the results remained consistent with the previous experiments, so the conclusion about the contribution of the hydroxide to the negative charge transfer was excluded. Further, three different oils were used to verify the universality of the phenomenon, and the results are shown in Figure S9 (Supporting Information), when all three kinds of oil droplets were initially positively charged, the positive charge of the droplets decrease dramatically after contacting with DI-water droplets, while the charge remained almost unchanged when oil were negatively charged. As mentioned above, assuming that the oil and water separation is incomplete, water droplet will take away a part of the oil. If the charge transfer is caused by material transfer, no matter the oil droplets are positively or negatively charged, the charges on the oil droplets will reduce significantly after contacting with water. Moreover, DI water could absorb both positive ions and negative ions, if the CE between the silicone oil and water was caused by ion adsorption, both the positive charges and negative charges could transfer from the silicone oil side to the DI water side. But in the experiments, when the oil droplets are negatively charged, the amount of negative charges will not significantly reduce before and after CE, but the positive charges will be greatly reduced. The contribution of material transfer and ions transfer to the charge transfer in L–L CE cannot support the above phenomenon. These results may indicate the existence of electron transfer in the CE between liquid and liquid. The difference in the behavior of positively and negatively charged oil droplet in the CE between silicone oil and DI water could be explained based on electron-cloud-potential-well model.^[27a] When the silicone oil droplet is negatively charged, the electrons are injected to the unoccupied orbitals of the silicone oil molecules. However, the highest occupied energy level (HOEL) of the charged silicone oil molecules still lower than that of the water molecules, or the electron still cannot overcome the potential barrier at the interface, therefore, no electron transfer from silicone oil side to the water side. If the silicone oil droplet is positively charged, the HOEL of silicone oil molecules will become lower and the potential barrier for electron transfer from water side to the silicone oil side will also become lower due to the electric field induced by the charges on the silicone oil surface. Therefore, electrons will be transferred from water droplet to silicone oil when it contacts with the DI water. The CE between a precharged water droplet and silicone oil was also investigated here, as shown in Figure 3c; and Movie S9 (Supporting Information). It is found that the transferred charges from water to the silicone oil side were limited, no matter the charges were positive or negative. This is because that the change of the HOEL of the water molecules induced by the extra charges is rather small. But it can still be noticed that negative charges are

much easier to transfer from DI water side to the silicone oil side, which may also support the existence of electron transfer in the CE between liquid and liquid (Figure 3c). Moreover, under the same induced electric field, water droplets are more easily to carry more positive charges compared to negative charges. The difference in the surface energy states density and HOEL of water, may be responsible for the phenomenon, when only considering the electron transfer model.

To further investigate the effect of applying electric field on liquid–liquid CE, as shown in Figure S10 (Supporting Information), Under the condition of applying voltage, the experiment of different charged types of oil droplets contacting with the water droplets was repeated. No matter whether the direction of the electric field is forward (Figure S8a–c, Supporting Information) or reverse (Figure S8d–f, Supporting Information), after contacting with the water droplet, the negative charge carried by negative oil (Figure S8c,f, Supporting Information) or positive charged oil (Figure S8b,e, Supporting Information) droplets always increases. Under applied electric field, the influence of ions transfer on the experiment is not obvious. The reason why for this situation is that the needle tip used to hang the droplet is grounded, and the strong potential difference between the needle tip and the electrode plate causes the electrons from the ground to be injected into the oil droplets through the water. Through the above experiments, it is difficult to judge the effect of ions in deionized water on the charge transfer, so three solutions were selected to measure the charge transfer under the condition of applying an electric field during liquid–liquid CE process, as shown in Figure S11 (Supporting Information). No matter whether the direction of the applied electric field is forward or reverse, after oil droplet being in contacting with droplets from different solutions, similarly, oil will be more negatively charged. But the difference is that the amount of charge transfer in different solutions is different, which may be related to the difference in migration of ions and electrons.

2.4. Effect of pH Value of the Aqueous Droplet on the CE between Liquid and Liquid

The pH value of the aqueous solution was demonstrated can affect the liquid–solid CE significantly.^[29] In order to further explore whether there are similar phenomena at the liquid–liquid interface, the CE between silicone oil droplet and aqueous solutions with different pH values was studied based on the acoustic levitation device. In the experiments, the precharged HCl solution droplets and NaOH solution droplets with different pH value were suspended by the acoustic device. And the charges of the aqueous droplets were measured before and after the contact with the silicone oil droplets, as shown in Figure 4. Figure 4a,b gives the results of the CE between the positively charged aqueous droplets and silicone oil, and Figure 4c,d gives that between negatively charged aqueous droplets and silicone oil. Here, the initial charges of the aqueous droplets were different, so that we calculated the charge transfer efficiency (T) for further analysis, which is defined as following

$$T = \frac{Q_i - Q_a}{Q_i} \quad (4)$$

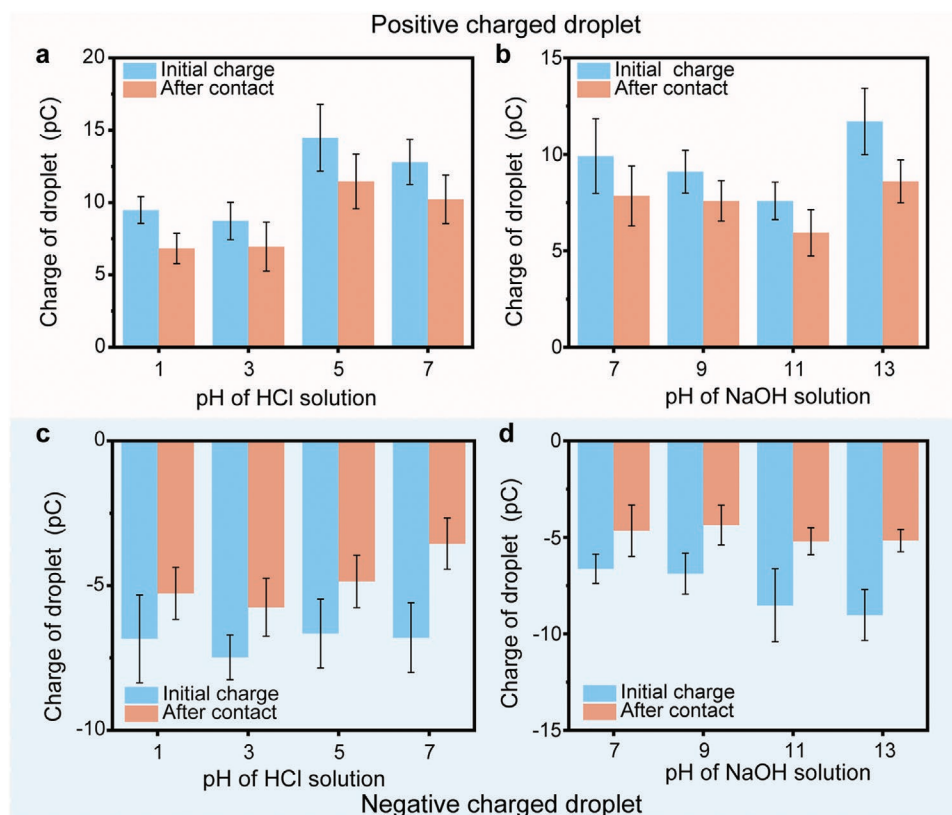


Figure 4. Effect of pH value on the CE between aqueous solutions and silicone oil. Charges on positively charged a) HCl droplet and b) NaOH droplet before and after contacting with silicone oil. Charges on negatively charged c) HCl droplet and d) NaOH droplet before and after contacting with silicone oil.

where the Q_i and Q_a denote the initial charges and the charges on the aqueous droplet after the CE.

The charge transfer efficiency in the CE between silicone oil and aqueous droplets are shown in Figure S12 (Supporting Information). It can be seen that the charge transfer efficiency in the CE between negatively charged aqueous droplets and silicone oil is always higher than that between positively charged droplet and silicone oil. This results also verify the asymmetrical behaviors of the positively precharged and negatively precharged oil droplet in the liquid–liquid CE, which further supports that electron transfer is the dominant charge transfer in liquid–liquid CE.

2.5. Charge Decay of the Aqueous Droplet During Evaporation

In addition to the CE between liquid–liquid CE, the acoustic levitation device can also be used to study the charge decay of the liquid droplet as a function of time. In the experiments, the aqueous droplets were first charged and suspended in the acoustic field. Then, the volume and the movement distance of the droplet in the acoustic field were recorded for a period time (0–6 min), as shown in Figure 5a,b, according to the volume and the movement distance of the droplets, the amount of charges of the droplets was calculated. The decay of the positively charged charges on the DI water droplet is shown

in Figure 5c,e. It turns out that the amount of charges on the DI water droplet will decay with the evaporation, no matter it is positive charges or negative charges, and both decay curves conform to the exponential decay model. It is generally believed that the main reason for the charge decay is that the dust particles in the air collide with the liquid droplets, which may neutralize the charge.^[30] In addition, as the water evaporates, both positive and negative charges will escape into the air from the surface of the liquid along with water molecules.^[31] Moreover, there is no obvious difference of the decay tendency between two charged types of droplets in the evaporation, but the rate of decay of the positive charge in the droplet is slightly greater than that of the negative charge. Different aqueous droplets with two charged types were used in this experiment, and the decay time was set to be 1.5 min, and the results are shown in Figure 5d,f. The decay of the charges on the aqueous droplet during evaporation is also observed, but the acid or base environment of the solution does not seem to have a great effect on the charge decay. To further investigate the effect of salt concentration on charge decay, as shown in Figure S13 (Supporting Information), NaCl solutions of different concentrations were naturally evaporated at room temperature. The results show that, under the same induction voltage, the droplet with higher salt concentration has more initial charges, and after 1.5 min of evaporation, the droplet with higher concentration has a greater change in the amount of charges.

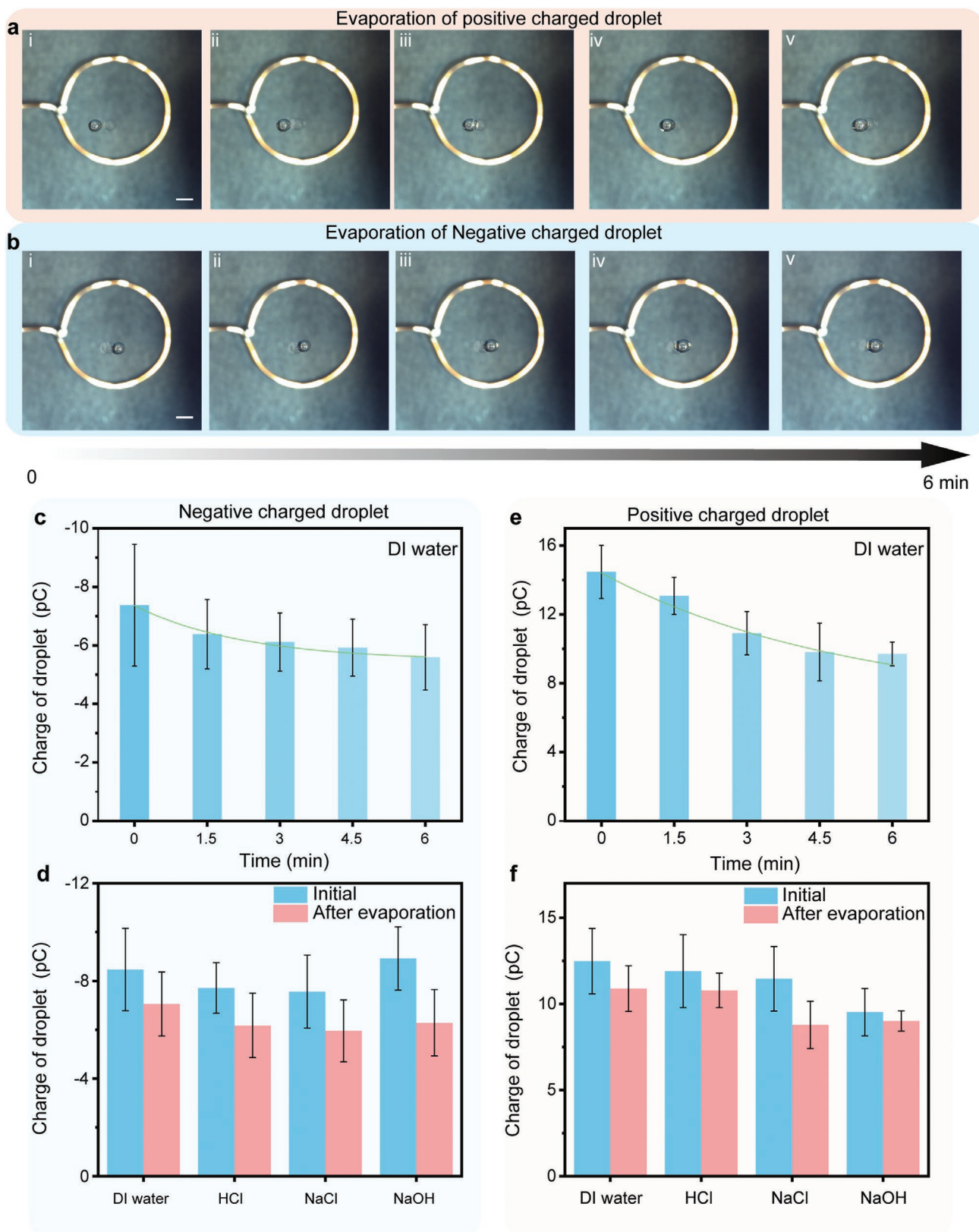


Figure 5. Measurement of the charge decay of the aqueous droplet during evaporation. photographs of a) positive charged and b) negative charged droplet evaporation process. The decay of the charges of c) negatively charged DI water droplet and d) other aqueous droplets. The decay of the charges of e) positively charged DI water droplet and f) other aqueous droplets. All experiments were performed in room environment, 27 °C and 17% humidity. Error bars represent the standard deviation of ten measurements. Scale bar: 2 mm.

3. Conclusion

In summary, a contactless method for quantifying the charges of the liquid droplets was designed based on the combination electric field and acoustic field. Both the liquid–solid and liquid–liquid CE were studied by using the method. In the liquid–solid CE, the transferred charges between the solid spheres and the aqueous droplets were found to decrease with the increasing of the ion concentration of the aqueous droplets, which is consistent with previous studies. We focus on the liquid–liquid CE and the CE between the silicone oil droplet and different aqueous droplets, including DI water droplet, NaCl droplet, HCl droplet, and NaOH droplet. It was found that the amount of positive charges transfer from a prepositively charged aqueous droplet to a silicone oil droplet is less than that of negative charges transfer from a prenegatively charged aqueous droplet to a silicone oil droplet. This phenomenon provides a strong evidence for the existing of electron transfer in the liquid–liquid CE. Moreover, the contactless measurement method was demonstrated to have more implications in the studies of the charging behavior in the liquid droplets, such as the decay of charges during the evaporation of the aqueous droplets. It also provides significant support for guiding the mechanism of TENG based on solid–liquid and liquid–liquid interfaces.

4. Experimental Section

Preparations for Samples: PTFE ball was purchased from Alibaba, the diameter of the ball is around 2.4–2.5 mm. Using extremely little glue to adhere a metal wire with a length of 3 cm and a diameter of 0.5 mm as a prop to the PTFE ball. All PTFE balls were cleaned with deionized water and ethanol. Ecoflex was purchased from commercial market. First, the ingredients A and B were poured into the container in a ratio of 1:1, the clean PTFE ball are immersed in container, and then, the PTFE ball with melted coated layer were pulled out, dried in a hot oven, and cooled to room temperature. A certain thickness of Ecoflex film deposited on the PTFE ball was achieved, and then it was cleaned by deionized water and ethanol. The bulk of paraffin was put into a vessel and heated, and the PTFE ball was immersed in the vessel when the paraffin was in liquid state. Since the melting temperature of paraffin is 58 °C, a uniform paraffin shell would naturally deposit on the cold PTFE surface. All of the samples were air-drenched under an ion fan for 10 min to eliminate the effect of surface charges on experiment.

Charging Process of Water Droplet: Using a clean microsyringe to draw the liquid from the different solutions, a wire was connected to the metal needle on the syringe, and connect the other end of this wire to the positive pole of the high-voltage power source, and connecting the negative pole of the power source to a hollow metal ring. Squeezing droplets at a feed rate of 5 μL each time, due to adhesion force, the droplet hangs on the tip of the needle, and droplet was placed close to the metal ring, but not touch it. By controlling the output of the high-voltage power supply, a corresponding amount of charge can be induced on the droplet.

Experimental Setup for Acoustic Levitation Device: The system consists of two parts: acoustic levitation part and electric field part. For acoustic levitation setup, the 72 ultrasonic transducers (MA40S4S, 40 kHz, 10 mm diameter) were divided into two groups, in which are arranged oppositely in a circular mold with a curvature of 6 cm and a distance of 117 cm from each other. Under 12 V input voltage, Arduino nano was used to generate square wave signals and L298N Dual H-bridge motor drive was to amplify the signals. When the transducer receives the square wave signal, it can apply sound radiation force to the objects in the sound

field. For electric field part, A pair of parallel plate capacitors are placed in the direction perpendicular to the x-axis of the acoustic field. The two ends of the parallel plate are, respectively, connected to the positive and negative poles of the high-voltage power supply. Here, the right end is defined as the positive pole. Parallel plate capacitors comprised of two 50 mm diameter copper plates, which provide a uniform electric field in the central space of $<8 \text{ mm}^3$ occupied by the droplets. The distance between the two plates is 38 mm.

Measurement for the Charges of Suspended Droplet: Using a microsyringe to suck liquid from different solutions, and slowly send the liquid with a volume of 5 μL into the desired position in the sound field each time. When the droplet is stably suspending in the sound field, a high voltage of 15 kV was applied on both sides of the parallel plate, and the distance the droplet moved toward the x-axis was recorded with a high-speed camera. Before and after the CE, the electric field was used to test the charge of the droplet, and charges difference between the two tests was used to determine the amount of charge transferred, and the influence of the initial charge of the droplet on the test was excluded. The OpenCV image analysis program was used to find the centroid of the droplet. The difference in displacement is determined based on the distance between the centroid before and after the droplet moves. The acoustic radiation force in the x-direction implement on the droplet at the position was calculated by the simulation software, therefore, the equilibrium relationship can be established to solve the corresponding electric field force at this time, and further calculate the charge amount of the droplet. The droplet size has been measured by pixel analysis from high-speed camera picture (see Figure S14, Supporting Information). The entire CE and measurement process are completed in a short time to avoid experimental errors caused by droplet evaporation. Errors in the measurements are mainly caused by oscillation of droplets after applied electric field.

Measurement for the Charge of Solid–Liquid, Liquid–Liquid Interface: For liquid–solid case, using a microinjection syringe to put the droplet into the acoustic field, and using insulated tweezers to clamp the metal rod, the small ball on that metal rod contacting with the suspended droplet. For L–L case, use a large-caliber syringe to put the precharged silicone oil (Aladdin, PMX200) drop into the acoustic field, and then use another water droplet attached on the needle of the syringe to contact the suspended oil drop, the needle with a water droplet is grounded. Another situation Use a microinjection syringe to put the precharged droplet into the acoustic field, A clean PTFE ball immersed dimethicone oil, and move the ball from the oil, due to the high viscosity of the dimethicone oil and strong adhesion, it will leave an oily film on the surface of PTFE, and using oil ball to contact with suspended water.

Evaporation of Droplets: Using the charging method mentioned above, 0.5 kV positive voltage and 3 kV negative voltage was used to charge droplets separately. Then put the droplet into the acoustic field, droplet will evaporate naturally, Under the experiment condition of 27 °C and relative humidity of 17%, electric field was used to detect the charge of droplets, and the displacement of liquid droplets was recorded by a high-speed camera. The device was placed in a Faraday cage made of acrylic and covered with a copper mesh to eliminate the influence of air flow and charged particles on the test.

Supporting Information

Supporting Information is available from the Wiley Online Library or from the author.

Acknowledgements

Z.T. and S.L. contributed equally to this work. S.L. and Z.L.W. conceived the idea. S.L. and Z.T. designed the experiments. Z.T. carried out the liquid–solid and liquid–liquid contact electrification experiments. Z.L.W. supervised the whole project. All the authors discussed the results and

contributed to the manuscript. The authors would like to thank LanXin Jia for grateful help to surface tensions tests. Research was supported by the National Key R & D Project from Minister of Science and Technology (No. 2016YFA0202704), National Natural Science Foundation of China (Grant No. 52005044).

Conflict of Interest

The authors declare no conflict of interest.

Data Availability Statement

Research data are not shared.

Keywords

acoustic levitation, charge transfer, contact electrification, electric field, triboelectric nanogenerators

Received: April 15, 2021

Revised: July 13, 2021

Published online:

-
- [1] J. Lowell, A. C. Rose-Innes, *Adv. Phys.* **1980**, *29*, 947.
- [2] a) F.-R. Fan, Z.-Q. Tian, Z. L. Wang, *Nano Energy* **2012**, *1*, 328; b) S. Niu, S. Wang, L. Lin, Y. Liu, Y. S. Zhou, Y. Hu, Z. L. Wang, *Energy Environ. Sci.* **2013**, *6*, 3576.
- [3] a) Y. S. Zhou, Y. Liu, G. Zhu, Z. H. Lin, C. Pan, Q. Jing, Z. L. Wang, *Nano Lett.* **2013**, *13*, 2771; b) S. Lin, L. Xu, C. Xu, X. Chen, A. C. Wang, B. Zhang, P. Lin, Y. Yang, H. Zhao, Z. L. Wang, *Adv. Mater.* **2019**, *31*, 1808197; c) H. T. Baytekin, A. Z. Patashinski, M. Branicki, B. Baytekin, S. Soh, B. A. Grzybowski, *Science* **2011**, *333*, 308.
- [4] a) S. Lin, L. Xu, A. Chi Wang, Z. L. Wang, *Nat. Commun.* **2020**, *11*, 399; b) S. Lin, M. Zheng, J. Luo, Z. L. Wang, *ACS Nano* **2020**, *14*, 10733.
- [5] a) R. A. W. Dryfe, in *Advances in Chemical Physics*, Vol. 141 (Ed: S. A. Rice), John Wiley & Sons Inc, Hoboken, NJ **2009**, p. 153; b) G. Herzog, *Analyst* **2015**, *140*, 3888; c) V. Mareček, Z. Samec, *Curr. Opin. Electrochem.* **2017**, *1*, 133; d) J. Nauruzbayeva, Z. Sun, A. Gallo Jr., M. Ibrahim, J. C. Santamarina, H. Mishra, *Nat. Commun.* **2020**, *11*, 5285; e) J. C. Bird, W. D. Ristenpart, A. Belmonte, H. A. Stone, *Phys. Rev. Lett.* **2009**, *103*, 164502; f) W. D. Ristenpart, J. C. Bird, A. Belmonte, F. Dollar, H. A. Stone, *Nature* **2009**, *461*, 377.
- [6] J. Nie, Z. Wang, Z. Ren, S. Li, X. Chen, Z. L. Wang, *Nat. Commun.* **2019**, *10*, 2264.
- [7] a) R. A. Millikan, *Science* **1910**, *32*, 436; b) R. C. Jones, *Am. J. Phys.* **1995**, *63*, 970.
- [8] a) S. B. Q. Tran, P. Marmottant, P. Thibault, *Appl. Phys. Lett.* **2012**, *101*, 114103; b) D. Foresti, M. Nabavi, M. Klingauf, A. Ferrari, D. Poulidakos, *Proc. Natl. Acad. Sci. USA* **2013**, *110*, 12549; c) Y. Ochiai, T. Hoshi, J. Rekimoto, *PLoS One* **2014**, *9*, e97590.
- [9] a) Z. Chen, D. Zang, L. Zhao, M. Qu, X. Li, X. Li, L. Li, X. Geng, *Langmuir* **2017**, *33*, 6232; b) M. Agthe, T. S. Plivelic, A. Labrador, L. Bergstrom, G. Salazar-Alvarez, *Nano Lett.* **2016**, *16*, 6838.
- [10] a) C. Mu, J. Wang, K. M. Barraza, X. Zhang, J. L. Beauchamp, *Angew. Chem., Int. Ed. Engl.* **2019**, *58*, 8082; b) A. Saha, S. Basu, C. Suryanarayana, R. Kumar, *Int. J. Heat Mass Transfer* **2010**, *53*, 5663.
- [11] A. G. Kline, M. X. Lim, H. M. Jaeger, *Rev. Sci. Instrum.* **2020**, *91*, 023908.
- [12] V. Lee, N. M. James, S. R. Waitukaitis, H. M. Jaeger, *Phys. Rev. Mater.* **2018**, *2*, 035602.
- [13] R. T. Hilger, M. S. Westphall, L. M. Smith, *Anal. Chem.* **2007**, *79*, 6027.
- [14] a) A. Marzo, S. A. Seah, B. W. Drinkwater, D. R. Sahoo, B. Long, S. Subramanian, *Nat. Commun.* **2015**, *6*, 8661; b) A. Marzo, B. W. Drinkwater, *Proc. Natl. Acad. Sci. USA* **2019**, *116*, 84.
- [15] a) L. P. Gorkov, *Dokl. Akad. Nauk SSR* **1961**, *140*, 88; b) H. Bruus, *Lab Chip* **2012**, *12*, 1014.
- [16] a) A. Marzo, T. Corkett, B. W. Drinkwater, *IEEE Trans. Ultrason. Ferroelectr. Freq. Control* **2018**, *65*, 102; b) A. Marzo, A. Barnes, B. W. Drinkwater, *Rev. Sci. Instrum.* **2017**, *88*, 085105.
- [17] a) Y. M. Jung, H. C. Oh, I. S. Kang, *J. Colloid Interface Sci.* **2008**, *322*, 617; b) J. G. Kim, D. J. Im, Y. M. Jung, I. S. Kang, *J. Colloid Interface Sci.* **2007**, *310*, 599.
- [18] D. Choi, H. Lee, D. J. Im, I. S. Kang, G. Lim, D. S. Kim, K. H. Kang, *Sci. Rep.* **2013**, *3*, 2037.
- [19] a) W. Xu, H. Zheng, Y. Liu, X. Zhou, C. Zhang, Y. Song, X. Deng, M. Leung, Z. Yang, R. X. Xu, Z. L. Wang, X. C. Zeng, Z. Wang, *Nature* **2020**, *578*, 392; b) P. Jiang, L. Zhang, H. Guo, C. Chen, C. Wu, S. Zhang, Z. L. Wang, *Adv. Mater.* **2019**, *31*, 1902793; c) H. Wu, N. Mendel, S. van der Ham, L. Shui, G. Zhou, F. Mugele, *Adv. Mater.* **2020**, 2001699.
- [20] H. Zou, Y. Zhang, L. Guo, P. Wang, X. He, G. Dai, H. Zheng, C. Chen, A. C. Wang, C. Xu, Z. L. Wang, *Nat. Commun.* **2019**, *10*, 1427.
- [21] a) Z. H. Lin, G. Cheng, L. Lin, S. Lee, Z. L. Wang, *Angew. Chem., Int. Ed. Engl.* **2013**, *52*, 12545; b) M. A. Brown, A. Goel, Z. Abbas, *Angew. Chem., Int. Ed. Engl.* **2016**, *55*, 3790.
- [22] a) F. Zhan, A. C. Wang, L. Xu, S. Lin, J. Shao, X. Chen, Z. L. Wang, *ACS Nano* **2020**, *14*, 17565; b) J. Nie, Z. Ren, L. Xu, S. Lin, F. Zhan, X. Chen, Z. L. Wang, *Adv. Mater.* **2020**, *32*, 1905696.
- [23] P. L. Marston, D. B. Thiessen, *Ann. N. Y. Acad. Sci.* **2004**, *1027*, 414.
- [24] T. P. Silverstein, *J. Chem. Educ.* **1998**, *75*, 748.
- [25] J. D. Smith, R. Dhiman, S. Anand, E. Reza-Garduno, R. E. Cohen, G. H. McKinley, K. K. Varanasi, *Soft Matter* **2013**, *9*, 1772.
- [26] F. Schellenberger, J. Xie, N. Encinas, A. Hardy, M. Klapper, P. Papadopoulos, H. J. Butt, D. Vollmer, *Soft Matter* **2015**, *11*, 7617.
- [27] a) Z. L. Wang, A. C. Wang, *Mater. Today* **2019**, *30*, 34; b) M. Willatzen, L. C. Lew Yan Voon, Z. L. Wang, *Adv. Funct. Mater.* **2020**, *30*, 1910461.
- [28] E. Poli, K. H. Jong, A. Hassanali, *Nat. Commun.* **2020**, *11*, 901.
- [29] R. Raiteri, S. Martinoia, M. Grattarola, *Biosens. Bioelectron.* **1996**, *11*, 1009.
- [30] a) H. Y. Erbil, *Adv. Colloid Interface Sci.* **2012**, *170*, 67; b) M. Roulleau, M. Desbois, *J. Atmos. Sci.* **1972**, *29*, 565; c) A. L. Yarin, G. Brenn, O. Kastner, D. Rensink, C. Tropea, *J. Fluid Mech.* **1999**, *399*, 151.
- [31] N. N. Barthakur, N. P. Arnold, *Int. J. Biometeorol.* **1995**, *39*, 29.